PAPER

Size-dependent dynamic characteristics of graphene based multi-layer nano hetero-structures

To cite this article: Y Chandra *et al* 2020 *Nanotechnology* **31** 145705

IOP Publishing Nanotechnology
Nanotechnology 31 (2020) 145705 (15pp) https://doi.org/10.1088/1361-6528/ab6231

Size-dependent dynamic characteristics of graphene based multi-layer nano hetero-structures

Y Chandra[1], T Mukhopadhyay[2], S Adhikari[1] and Ł Figiel[3]

[1] Zienkiewicz Centre for Computational Engineering, Swansea University, Swansea SA1 8EN, United Kingdom
[2] Department of Aerospace Engineering, Indian Institute of Technology Kanpur, Kanpur, India
[3] International Institute for Nanocomposite Manufacturing (IINM) & Warwick Center for Predictive Modelling (WCPM), University of Warwick, CV4 7AL, United Kingdom

E-mail: tanmoy@iitk.ac.in

Received 19 July 2019, revised 11 November 2019
Accepted for publication 16 December 2019
Published 16 January 2020

Abstract

Carbon-based nano hetero-structures are receiving increasing attention due their ability in multi-synchronous modulation of a range of mechanical and other critically desirable properties. In this paper, the vibration characteristics of two different graphene based heterostructures, graphene-hexagonal boron nitride (hBN) and graphene-molybdenum disulfide (MoS_2), are explored based on atomistic finite element approach. Such vibrational characteristics of nanostructures are of utmost importance in order to access their suitability as structural members for adoption in various nano-scale devices and systems. In the current analysis, the developed atomistic finite element model for nano-heterostructures is extensively validated first with the results available in literature considering elastic responses and natural frequencies. Thereafter a range of insightful new results are presented for the dynamic behaviour of various configurations of graphene-hBN and graphene-MoS_2 heterostructures including their size, chirality and boundary dependence. The investigation of tunable vibrational properties along with simultaneous modulation of other mechanical, electronic, optical, thermal and chemical attributes of such nano-heterostructures would accelerate their application as prospective candidates for manufacturing nanosensors, electromechanical resonators, and a wide range of other devices and systems across the length-scales.

Keywords: 2D materials, dynamics of heterostructures, hexagonal nano-structures, atomistic finite element, graphene, hexagonal boron nitride, molybdenum disulfide

(Some figures may appear in colour only in the online journal)

1. Introduction

Since the discovery of superlative monolayers and thin films of graphite [1, 2], research interest in the engineering and scientific applications of carbon nanostructures has been growing exponentially due to their prospective unprecedented multi-functional applications in a range of nanoelectromechanical systems and devices. The superlatives identified in graphene have also led to an increased interest in other possible two-dimensional (2D) materials that could offer exceptional electronic, optical, thermal, chemical and mechanical characteristics [3–6]. Since the last decade curiosity in quasi-two-dimensional family of nano materials has grown from hexagonal boron nitride (hBN), boron–carbon–nitride (B–C–N), graphene oxides, chalcogenides such as molybdenum disulfide (MoS_2), molybdenum diselenide ($MoSe_2$) to stanene, silicene, sermanene, phosphorene, borophene etc [7–10]. It is essential to investigate these materials at nanoscale since the superlative properties appear in atomic scale and in single or few layer forms [11]. 2D nano materials investigated in the literature are of various geometrical patterns and among these, hexagonally shaped (it is interesting to

note that hexagonal shapes exist in various other natural and artificially constructed structures across different length scales [12–18]) nano-structures are found in abundance [4, 10, 73]. Such single layer nano materials have been extensively investigated using *ab initio* calculations [19–21], molecular dynamics (MD) [22–24] and molecular mechanics (MM) [25–30] based approaches.

Though single layers of different 2D materials have shown exceptionally promising properties covering the electronic, optical, thermal, chemical and mechanical characteristics, they can not show multiple desirable properties in a single nanostructure. For example, MoS_2 is rich in electronic and piezoelectric properties, but this is mechanically so weak that it can not be used in the nanoelectromechanical devices. On the other hand, graphene is mechanically very strong. Thus it is possible to combine these two nanostructures to form a single heterostructure, where the electronic and piezoelectric properties as well as mechanical strength can be achieved. Considering the emergence of so many single layer 2D nanostructures with their diverse properties and possibility of combining them in different stacking sequences open up a whole new domain of research for developing nanostructures with tunable multi-synchronous properties (analogous to metamaterials [31, 32] at nanoscale). Besides the electronic, optical, thermal and chemical properties of heterostructures, recent studies can be found in literature focusing on their effective mechanical properties [33–36, 7, 37–39].

Vibrational characteristics of nanostructures are of utmost importance in order to access their performance as structural members for adoption in nano-scale devices and systems. However, barring a single investigation [40], the dynamics and vibration of nano-heterostructures have not received any attention yet. Thus here we aim to investigate the size-dependent dynamic behavior of nano hetero-structures in terms of natural frequencies and mode shapes by developing a generic atomistic finite element (FE) model. In this context, it can be noted that 2D material monolayers could have either all the atoms situated in a single plane (such as graphene, hBN), or the atoms may be situated in different planes (such as MoS_2), referred as monoplanar and multiplanar nanostructures respectively [10]. In this article, we would focus on two different forms of graphene based heterostructures by stacking graphene with both monoplanar (graphene-hBN) and multiplanar (graphene-MoS_2) structures (refer to figure 1).

Hereafter this paper is organised as follows. In the second section, the derivation for mechanical equivalence of atomic bonds is shown. This is followed by an overview of the atomistic simulation methodology utilized to model nano hetero-structures (third section). Here we describe the finite element based atomistic modelling of individual sheets of graphene, hBN, MoS_2 and the weak van der Waals interactions between them. The results and discussion are presented in the fourth section. The atomistic finite element model of the heterostructure is first validated against available results from literature considering two different mechanical properties, Young's modulus and natural frequency. After gaining adequate confidence on the atomistic finite element model through extensive validation, we have presented new results for detailed dynamic analysis of graphene-hBN and graphene-MoS_2 nano hetero-structures. The results investigate the influence size parameters (length, aspect ratio), boundary conditions and chirality on the natural frequencies and mode shapes of nano hetero-structures. In the final section, concluding remarks are given along with a perspective of the current analysis.

2. Mechanical equivalence of atomic bonds

In case of the atomic scale behaviour of materials, total inter-atomic potential energy can be expressed as a summation of various individual energy components relevant to bonding and non-bonding atomic interactions [10, 25]. Total strain energy (E_E) can be represented as summation of the energy components from bond bending (E_b), stretching of bonds (E_s), bond torsion (E_t) and energies contributed by non-bonded terms (E_{nb}) like van der Waals attraction, core repulsions and coulombic energy

$$E_E = E_s + E_b + E_t + E_{nb}. \tag{1}$$

The influence of stretching and bending is significant in case of small deformations as compared to all other energy components [27, 41]. For the case of hexagonal multiplanar structures (like MoS_2), the strain energy due to bending is contributed by two different components, in-plane (E_{bI}) and out-of-plane (E_{bO}) [10]. The deformation mechanisms for the multiplanar nanostructure (like MoS_2) are shown in figures 2–3. The out-of-plane angular component reduces to zero for monoplanar structures (like graphene and hBN). The total inter-atomic potential energy (E_E) can be expressed as

$$\begin{aligned} E_E &= E_s + E_{bI} + E_{bO} \\ &= \frac{1}{2}k_r(\Delta l)^2 + \left(\frac{1}{2}k_\theta(\Delta\theta)^2 + \frac{1}{2}k_\theta(\Delta\alpha)^2\right), \end{aligned} \tag{2}$$

where Δl, $\Delta\theta$ and $\Delta\alpha$ are the variation in bond length, variation in in-plane angle and variation in out-of-plane angle respectively (refer to figure 2). The parameters k_r and k_θ are the force constants associated with bond stretching and bending respectively. The first term in equation (2) represents strain energy relevant to stretching (E_s), while the other terms represent the strain energies contributed by in-plane (E_{bI}) and out-of-plane (E_{bO}) angle deformation, respectively.

The force constants of atomic bonds (k_r and k_θ), as described above, can be expressed in the form of structural mechanics equivalence [72]. As per classical structural mechanics theory (refer to figure 3), strain energy of a uniform circular beam with length l, cross-sectional area A, second moment of area I and Young's modulus E under pure axial force N (refer to figure 3(b)) can be expressed as

$$U_a = \frac{1}{2}\int_0^L \frac{N^2}{EA}\,\mathrm{d}l = \frac{1}{2}\frac{N^2 l}{EA} = \frac{1}{2}\frac{EA}{l}(\Delta l)^2. \tag{3}$$

The strain energies due to pure bending moment M (refer to

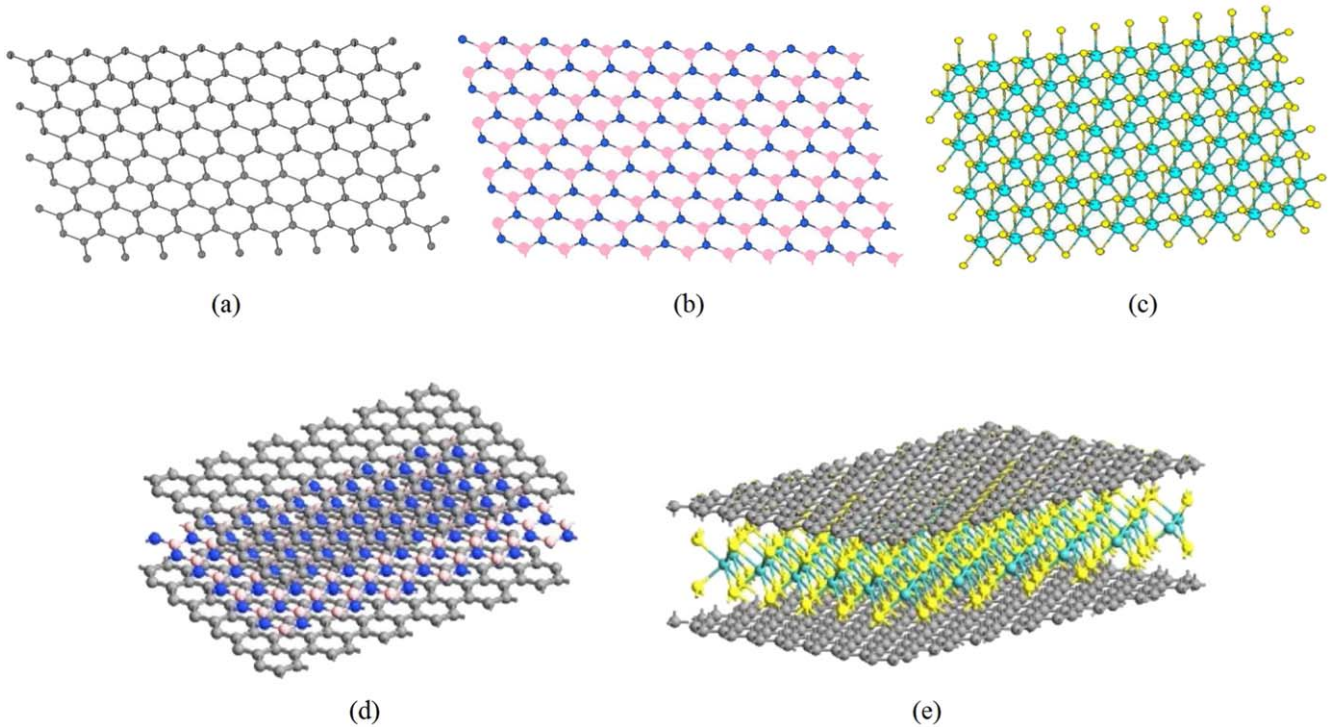

Figure 1. Isometric views of nanostructures and heterostructures. (a) Graphene (monoplanar nanostructure) (b) hBN (monoplanar nanostructure) (c) MoS_2 (multiplanar nanostructure, refer to figure 2(a) for further structural details) (d) Graphene-hBN heterostructure (hBN layer sandwiched between two graphene layers) (e) Graphene-MoS_2 heterostructure (MoS_2 layer sandwiched between two graphene layers). Black dots:carbon atoms, pink dots: boron atoms, blue dots: nitrogen atoms, aqua dots: molybdenum atoms and yellow dots: sulphur atoms.

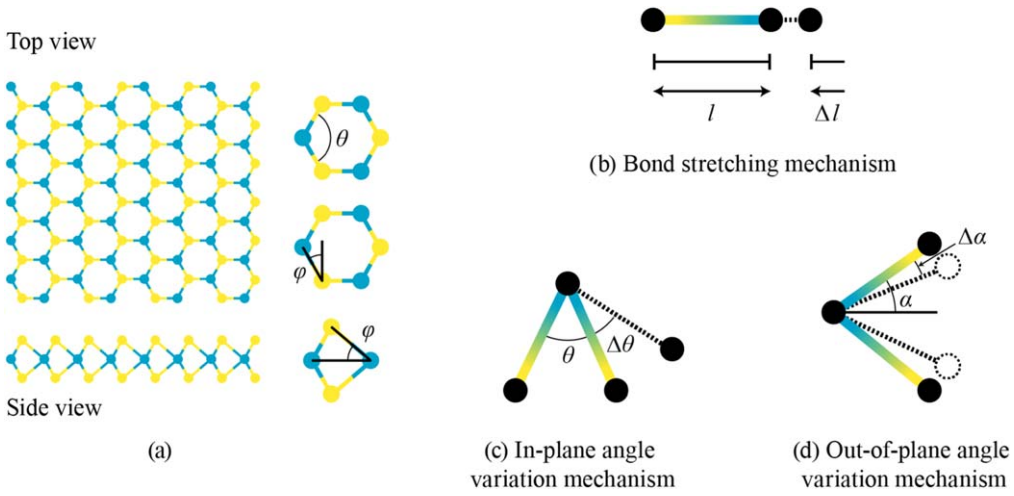

Figure 2. (a) Top and side views of a multiplanar hexagonal nanostructure such as MoS_2 (b) Bond stretching induced strain energy (c) In-plane angle variation induced strain energy (d) Out-of-plane angle variation induced strain energy.

figure 3(c)) can be written as

$$U_b = \frac{1}{2}\int_0^L \frac{M^2}{EI}\,\mathrm{d}l = \frac{1}{2}\frac{EI}{l}(2\Delta\phi)^2. \tag{4}$$

Comparing equation (3) with (2) for the expression of strain energy due to stretching (E_s), it can be concluded that $K_r = \dfrac{EA}{l}$. As per figure 3(c), it is reasonable to assume for bending that $2\Delta\phi$ is equivalent to $\Delta\theta$ and $\Delta\alpha$ for in-plane and out-of-plane angle deformations respectively. Thus comparing equation (4) with the expressions for the strain energies due to in-plane (E_{bI}) and out-of-plane (E_{bO}) angle deformations (refer equation (2)), the following equivalence can be obtained: $k_\theta = \dfrac{EI}{l}$. Such mechanical equivalence between molecular mechanics parameters (k_r and k_θ) and structural mechanics parameters (EA and EI) can be used to derive beam (covalent bond) properties used in the atomistic simulations. In the current work, the effective elastic moduli and natural frequencies of nano hetero-structures are computed by using these beams representing covalent bonds.

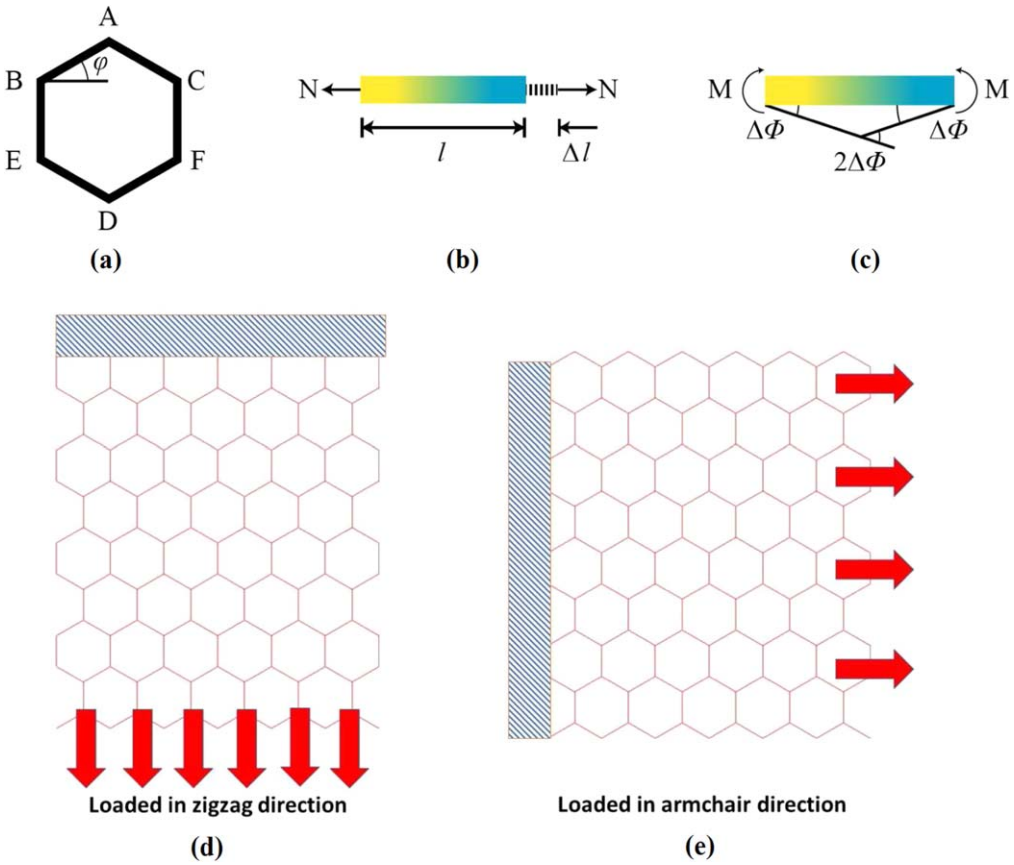

Figure 3. (a) A hexagonal unit cell involving of 6 idealized beam elements (refer to figure 2(a)) (b) A beam element under the influence of pure tension (c) A beam element under the influence pure bending (d)–(e) Boundary conditions for elastic analysis of the entire 2D material monolayers and their heterostructures (The marked edges are fully constrained in all six degrees of freedom).

Table 1. Bond angles and sheet thickness for nano materials [10]. Refer figure 2 for angle representations.

Nanomaterial	α (in ^{o})	θ (in ^{o})	Sheet thickness (nm)
Graphene	0	120	0.34
hBN	0	120	0.098
MoS_2	48.15	120	0.603

3. Atomistic finite element model of nano heterostructures

The concept of idealizing atomic bonds as equivalent beam elements, as presented in the preceding section, is utilized to model the nano-heterostructures in a finite element based framework [42–45]. It is the first ever attempt to develop any such atomistic finite element model for heterostructures, which could be a generic computationally efficient framework for characterizing the vibrational properties. In this research work, the finite element analysis tool OPTISTRUCT [46] has been used to model the dynamic behaviour of nano heterostructures. The covalent bonds are represented by 3D Timoshenko finite element beams and the atoms are represented by finite element nodes. Within the finite element analysis tool OPTISTRUCT, the element type CBEAM has been used to represent beams. The cross-sectional diameter and the Young's modulus (E) of the beam elements are computed by using the equations of force-field constants K_r(stretching) and K_θ(bending), as described in section 2.

The numerical values of force constants K_r and K_θ along with the necessary geometric attributes (bond lengths and bond angles) are shown in the tables 1–2 [10]. By substituting these values in the equations $K_r = \frac{EA}{l}$ and $k_\theta = \frac{EI}{l}$, essential parameters to model covalent bonds such as beam diameter d and beam Young's modulus E can be calculated. The calculated values of beam diameter and beam Young's modulus are shown in table 2, wherein it is evident that MoS_2 has the highest interatomic bond length, while graphene has the lowest bond length among the three materials considered in this work. The C–C bond length within graphene sheets is very close to that of B–N bond length in hBN sheets. Atomic masses of carbon, boron, nitrogen, molybdenum and sulphur have been considered by modeling mass elements on the nodes. The atomic masses considered here are 1.9943×10^{-26} kg, $1.7952086 \times 10^{-26}$ kg, $2.3258671 \times 10^{-26}$ kg, $1.593121X10^{-25}$ kg and $1.593121X10^{-23}$ kg for carbon, boron, nitrogen, molybdenum and sulphur, respectively. Within the finite element analysis tool OPTISTRUCT [46], the element type CONM2 has been used to represent masses.

Table 2. Bond properties for each individual nano material [10].

Nanomaterial	K_r in N nm^{-1}	K_θ in N nm rad^{-2}	L in nm	d in nm	E in GPa
Graphene	6.52e−7	8.76e−10	0.142	0.146	1370.91
hBN	4.86e−7	6.95e−10	0.145	0.151	1047.1
MoS_2	1.64e−7	1.67e−9	0.242	0.403	882.1

Table 3. Constants of L–J potentials.

Nanomaterial	ϵ in meV	σ in Å	Source
C–Mo	3.325	2.82	[35]
C–S	7.355	3.22	[35]
Mo–Mo	2.43	2.72	[36]
S–S	1.19	3.59	[36]
Mo–S	2.49	3.16	[36]
C–B	3.6	2.2132	[49]
C–N	9	3.2222	[49]
B–B	4.16	3.453	[50]
N–N	6.281	3.365	[50]

Interlayer interaction between two adjacent layers of a heterostructure can be modelled using Lennard–Jones (L–J) potential. The equivalent axial force for an L–J potential between pair of atoms (i, j) belonging to different nano layers is defined as [47]

$$F_{ij} = \frac{\partial V_{ij}}{\partial r}, \tag{5}$$

where r denotes the atomic displacement along ij (layer-layer length). The force between two atoms (ij) can also be expressed as [48]

$$F_{ij} = -12\,\epsilon\left[\left(\frac{r_{\min}}{y}\right)^{13} - \left(\frac{r_{\min}}{y}\right)^{7}\right] \tag{6}$$

where, $y = r_{\min} + \delta r$, and δr represents the atomic displacement along the length of **ij**. The quantity $r_{\min}$ (in Å) is given by $2^{\frac{1}{6}}\,\sigma$, where $\sigma = (A/B)^{1/6}$. The parameters B and A denote attractive and repulsive constants, respectively. In the current research work, three different nano sheets are considered namely graphene, hBN and MoS_2. Thereafter heterostructures of graphene-hBN and graphene-MoS_2 are studied under dynamic conditions. These hetero-structures lead to C–B, C–N, B–B, N–N, C–Mo, C–S, Mo–Mo, Mo–S and S–S atomic interactions, where C, B, N, Mo and S are carbon, boron, nitrogen, molybdenum and sulphide atoms, respectively. The values of σ and ϵ for each individual van der Waals atomic interactions are given in table 3. These values have been obtained from various references [35, 36, 49, 50]. In the atomistic FE simulations, we have modelled spring elements to obtain a nonlinear connection between two adjacent layers of a heterostructure representing the L–J interactions. The force-deflection curve for such L–J springs are calculated by using equation (6), as shown in figure 4. Within the finite element analysis tool OPTISTRUCT [46], the L–J springs of interlayer interactions are modeled by element type CBUSH incorporating the curves of figure 4 as input properties.

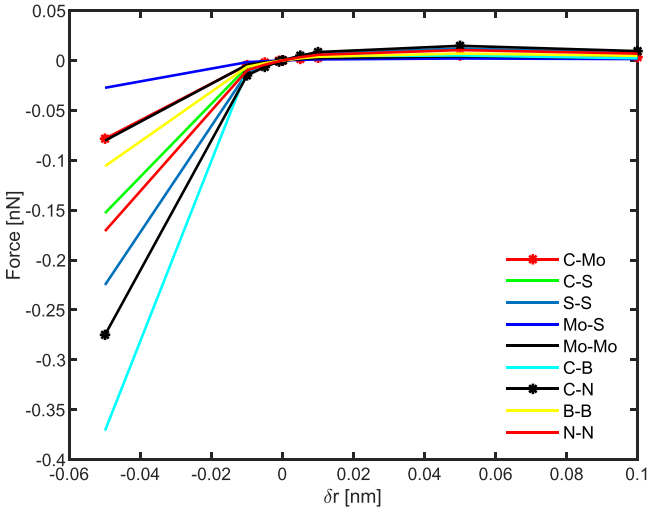

Figure 4. Curves of L–J potential forces obtained by equation (6).

In the atomistic FE approach, coupled nano sheets of heterogenous nature are modeled like space-frame structures. Overall stiffness and mass matrices of the atomistic FE models are obtained by assembling the equivalent matrices of the beams representing C–C, C–S, Mo–Mo, S–S, Mo–S, C–B, C–N, B–B and N–N bonds and the concentrated masses situated at each node. Here the lumped mass matrix in case of a single beam element can be expressed as:

$$[\mathbf{M}]_{\mathbf{e}} = diag\left[\frac{m_a}{n}\ \frac{m_a}{n}\ \frac{m_a}{n}\ 0\ 0\ 0\right] \tag{7}$$

where m_a (in kg) is the mass of atoms and n is the number of bonds attached to an atom in the nanosheet. To obtain the natural frequencies and mode shapes of nano-hetero-structures, the general equation of motion of an undamped system ($[\mathbf{K}]\mathbf{x} + [\mathbf{M}]\ddot{\mathbf{x}} = 0$) leading to the standard eigenvalue problem ($([\mathbf{K}] - \omega^2[\mathbf{M}])\{\mathbf{x}\} = \{\mathbf{0}\}$) can be solved using Block Lanczos algorithm [51] within the atomistic finite element analysis code [46].

4. Results and discussion

Here we start by validating the developed atomistic finite element model of heterostructures using two different mechanical properties, Young's modulus and natural frequency. After gaining adequate confidence on the proposed model, insightful new results are presented for the dynamic behaviour of graphene based heterostructures including the effect of size, boundary condition and chirality.

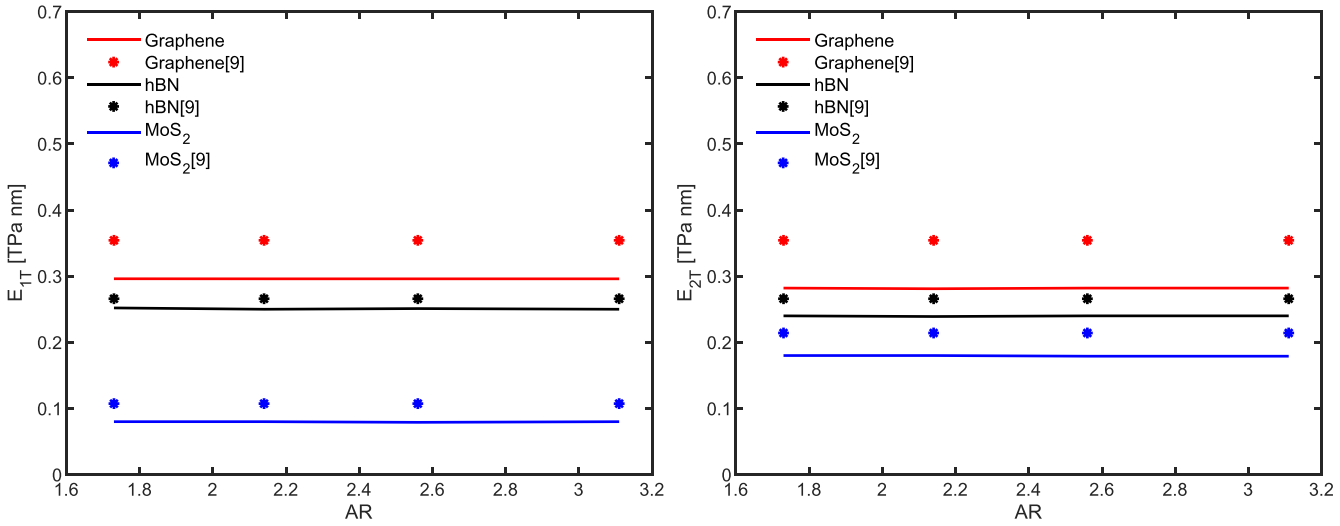

(a) Tensile rigidity in armchair direction (b) Tensile rigidity in zigzag direction

Figure 5. Variation of tensile rigidity against aspect ratio (AR). The results obtained using the current atomistic FE simulations are validated against literature [10].

4.1. Validation of Young's modulus (E) of graphene, hBN and MoS_2

In this subsection, the Young's modulus of graphene, hBN and MoS_2 has been obtained using the atomistic finite element method and compared with the corresponding values available in literature. For each nano material, the elastic analysis has been performed in zigzag and armchair directions. With respect to armchair and zigzag directions, one end of the nano sheet has been constrained and an unit load has been applied to the other end. The unit load has been introduced through a rigid element (multi point constraint) connected to the group of nodes at the end of nanosheet. These boundary conditions are depicted in figures 3(d)–(e). The resulting strain due to the applied unit load has been numerically calculated using the atomistic FE simulations. Based on this strain and applied stresses due to the unit load, the Young's modulus of the 2D materials has then been obtained. Here the Young's modulus with respect to armchair direction is referred as E_1 and that with respect to zigzag direction is referred as E_2. The Young's moduli E_1 and E_2 have been converted to tensile rigidities E_{1T} and E_{2T} by multiplying the corresponding modulus with the sheet thickness shown in the table 1.

For the case of graphene and hBN sheets, four separate finite element models have been constructed with sheet sizes 1.775 nm × 3.074 nm, 1.775 nm × 3.813 nm, 1.775 nm × 4.55 nm and 1.775 nm × 5.534 nm. The largest among these four finite element models has resulted in upto 654 beam elements and 513 nodes. The aspect ratio (AR) of these four finite element models are 1.73, 2.14, 2.56 and 3.11. Also, for the case of MoS_2 sheets, 4 separate finite element models have been constructed with sheet sizes 1.483 nm × 2.625 nm, 1.483 nm × 2.94 nm, 1.483 nm × 3.359 nm and 1.483 nm × 4.199 nm. The largest among these four finite element models has resulted in upto 958 beam elements and 587 nodes. The AR of these four finite element models are 1.77, 1.98, 2.26 and 2.83. The variation of E_{1T} and E_{2T} against AR for all three nano materials are shown in figure 5. Within these plots, are also presented the E_{1T} and E_{2T} obtained from literature [10]. The authors [10] considered an analytical closed-form formula to determine unique values of E_{1T} and E_{2T} of graphene, hBN and MoS_2 by considering a single hexagonal unit cell of each nano material. Due to this fact, the curves from the literature [10] remain flat in the plots of figure 5. As per these plots, the numerically predicted values are quite close to that of the analytical prediction of literature. However, the current values are found be slightly lower as compared to the analytical predictions of literature. This can be attributed to the fact that the analytical predictions are based on a single unit cell, where the shear deformations were neglected. In the current numerical analysis shear based deformation is allowed in the lattice system considering Timoshenko finite element beams, leading to more flexibility in the nanosheets. Moreover, within the atomistic finite element simulations multiple number of unit cells in each sheet are considered, resulting in a high number of beam elements. As the number of beam elements increases, more flexibility is added to the model. The cumulative effect of such flexibility can underpredict the elastic modulus of the nano structures. The variation of tensile rigidities with respect to AR is found to be negligible in figure 5. At larger ARs (>10), the values of tensile rigidities increase slightly (<1%). Furthermore, the numerically obtained single layer tensile rigidities have also been compared against the results from various other publications covering *ab initio* calculations, molecular dynamic simulations and experimental investigations (refer to table 4). From the results presented in this subsection, it can be concluded that the tensile rigidities calculated using the atomistic FE model are in good agreement with the numerical values available in literature, corroborating the validity of the

Table 4. Results for Young's moduli in the form of tensile rigidity(E_T) compared against the values from literature. E_{1T} and E_{2T} are tensile rigidities in two directions taken from the current work. Similar to the present results, Mukhopadhyay *et al* [10] reported different values of Young's modulus in the longitudinal and transverse directions of MoS_2.

Material	Present results (TPa nm)	Reference results from literature (E_T in TPa nm)
Graphene	$E_{1T} = 0.296$ $E_{2T} = 0.282$	Experimental: 0.34 [55], 0.306 [52] *Ab initio*: 0.350 [56], 0.357 [21], 0.377 [57], 0.364 [58] Molecular dynamics: 0.357 [59], 0.343 [60] Molecular mechanics: 0.354 [27], 0.3604 [25], 0.354 [10]
hBN	$E_{1T} = 0.252$ $E_{2T} = 0.240$	Experimental: 0.251 [53] *Ab initio*: 0.271 [56], 0.272 [61] Molecular dynamics: 0.236 [62], 0.278 [63] Molecular mechanics: 0.269 [64], 0.322 [65], 0.265 [10]
MoS_2	$E_{1T} = 0.080$ $E_{2T} = 0.180$	Experimental: 0.211 [66], 0.163 [54] *Ab initio*: 0.141 [67], 0.262 [68] Molecular dynamics: 0.150 [69] Molecular mechanics: 0.107 (E_{1T}) and 0.214 (E_{2T}) [10]

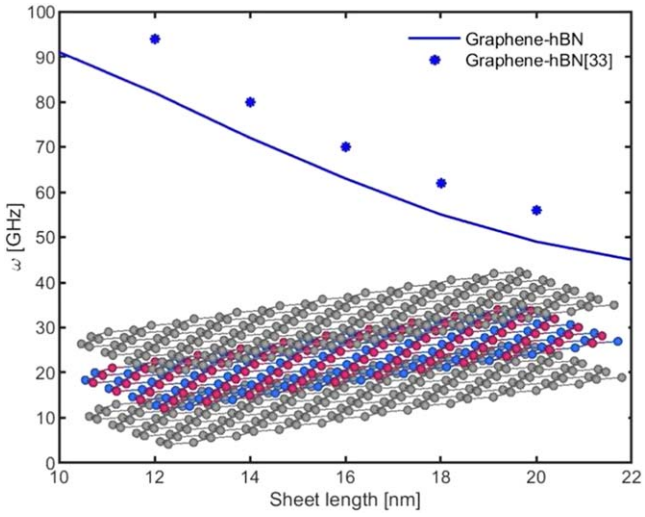

Figure 6. Comparison of natural frequency of current work against the values available in literature [40]. A schematic representation of the considered heterostructure is shown in the inset, wherein the two outer layers are graphene and the middle layer is hBN.

developed computational model. In the table 4, for the case of graphene, the current approach predicted tensile rigidity ($E_{1T} = 0.296$ TPa nm) close to that of experimental work [52] (0.306 TPa nm). For the case of hBN and MoS_2, the current predicted tensile rigidity values are also found to be close to that of experimental works [53, 54]. Such a close correlation indicate that the present numerical results agree very well with experimental works obtained under more realistic conditions. The discrepancies between the current numerical results, and the MM/MD based results can be due to various reasons such as omission of non bonded energy terms in equation (1) and presence of degrees of freedom including shearing effect within the Timoshenko finite elements representing covalent bonds.

4.2. Validation of natural frequencies of nano-heterostructures

After validating the developed atomistic finite element model with respect to the Young's moduli of 2D materials, here we present a further verification/validation for the dynamic behaviour of nano-heterostructures considering a combination of graphene and hBN. This section involves dynamic analysis of graphene-hBN triple layer nano hetero-structure, wherein alternating graphene and hBN sheets have been overlapped into three layers. This configuration has been chosen to validate the present numerical model against the MD model of similar configuration available in literature [40]. In order to validate the atomistic FE dynamic models, the modal analysis has been performed by constraining two edges of the multi-layer nano-heterostructures. Four separate finite element models have been constructed with sheet sizes 5.534 nm × 12.121 nm, 5.534 nm × 13.789 nm, 5.534 nm × 18.101 nm and 5.534 nm × 20.112 nm. For these four finite element models, the width has been kept constant at 5.534 nm and the length has been varied from 12.121 nm to 20.112 nm. These dimensions, boundary conditions and layer combinations have been chosen in order to replicate the MD simulations available in literature [40].

The variation of the natural frequency with respect to the sheet lengths is shown in figure 6. This plot presents two curves, a curve from the current atomistic FE simulations and a curve extracted from the MD results [40]. The trend of variation in the current work is comparable with that of the MD simulation [40]. Both atomistic FE and MD simulations predict a drop in natural frequency as the length of multilayer nano hetero-structure sheet is increased. However, the natural frequencies predicted by the atomistic FE simulations are found to be lower than those predicted by MD simulations. This is due to the fact that the number of numerical approximations happening within the finite element analysis including round off approximations and beam element six degrees of freedom (leading to sheet flexibility). Other

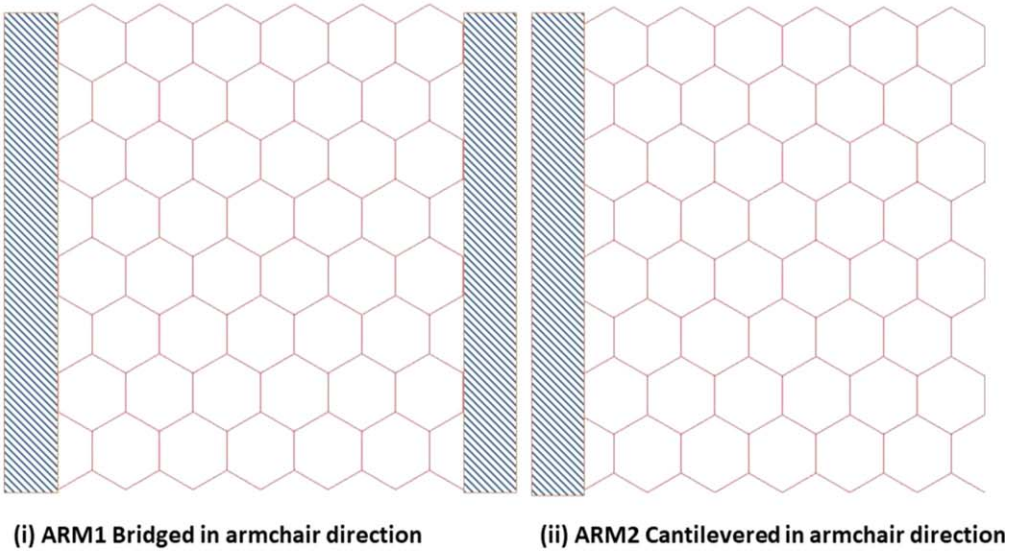

(a) Bridged and Cantilevered in armchair direction

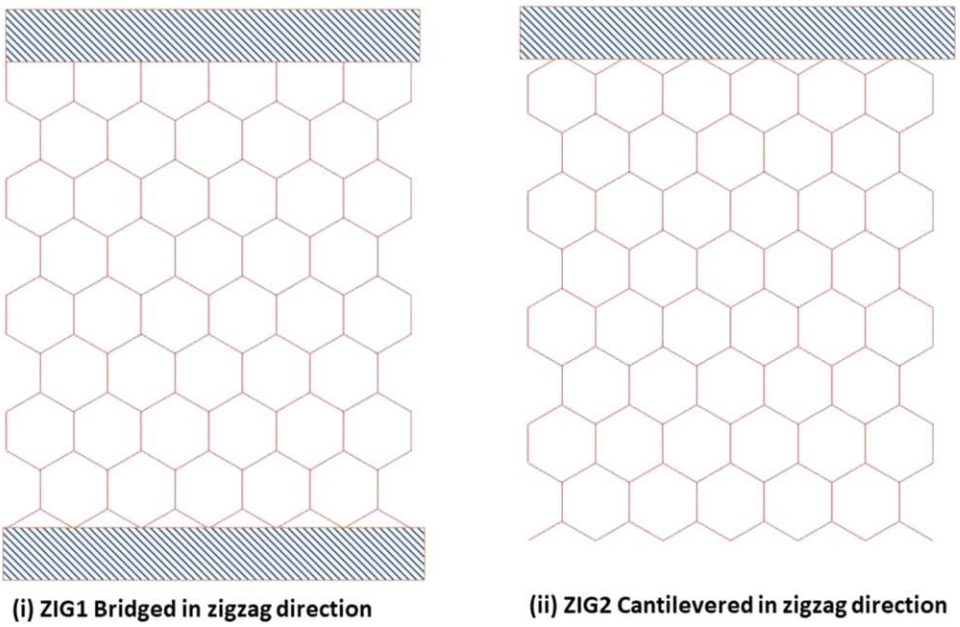

(b) Bridged and Cantilevered in zizag direction

Figure 7. Depiction of bridged and cantilever boundary conditions (the marked edges are fully constrained in all six degrees of freedom).

reasons such as omission of non bonded energy terms in equation (1) and shearing effect within the Timoshenko beam finite elements can also contribute to such discrepancies. At higher lengths, the results of atomistic FE simulations tend to converge towards those of MD simulations. Also, the curve of natural frequency between the lengths 18.101nm and 20.112 nm appears to be relatively flat as compared to the rest of the curve. This further proves that, as the atomistic space frame lattice of nano-structures becomes larger in dimension, it simulates a continuous plate similar to earlier reports for bilayer and single layer graphene sheets [45]. It can be noted that the results presented in sections 4.1 and 4.2 comprehensively establish the validity and confidence in the developed atomistic FE model. Hereafter new results on the dynamic behaviour of graphene based heterostructures are presented following the developed computational model.

4.3. Higher order modal behaviour of nano hetero-structures

In this subsection we have studied three higher order modes of nano-heterostructures except the first mode of vibration. To understand the nature of dynamic features, mode shapes are required to be studied for a complex system. In order to demonstrate the mode shapes associated with natural

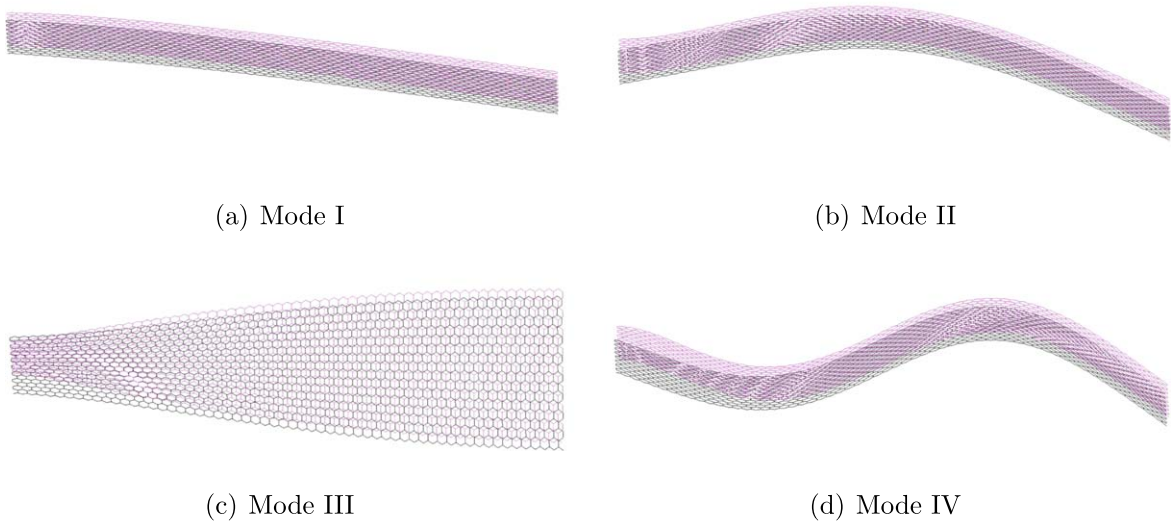

Figure 8. First four mode shapes of graphene-hBN nano hetero-structure.

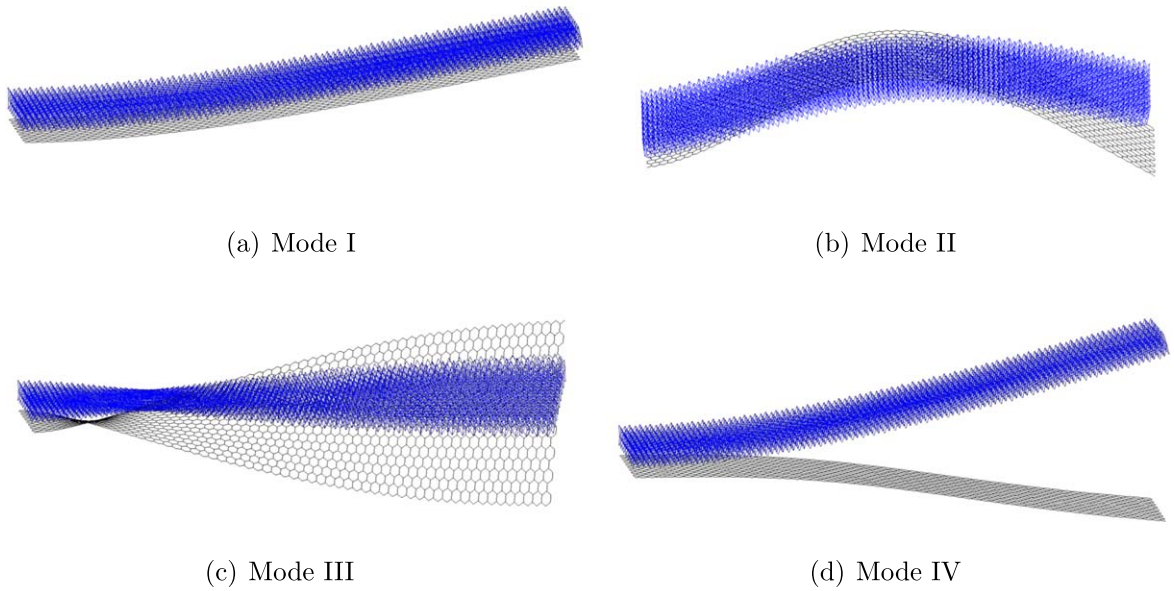

Figure 9. First four mode shapes of graphene-MoS_2 nano hetero-structure.

frequencies, the 1st four mode shapes are presented in this section. Prior to enforcing boundary conditions, an initial free-free modal simulation has been carried out to verify the dynamic behaviour of the double layer structures without the influence of external clamps and/or supports. A free-free run involves extracting and verifying rigid body mode shapes without any constraints, in order to ensure the integrity of the structure. The boundary condition used to perform modal analysis is cantilevered condition (figure 7). Cantilever condition involves clamping at one-edge and setting free other three edges of the nanostructures. Modal analysis has been performed on graphene-hBN and graphene-MoS_2 nano hetero-structures. Chosen size of both heterostructures is 10.5 nm × 3.5 nm. Such a dimension will lead to a nano ribbon type rectangular sheet with an AR 3. The first four mode shapes for graphene-hBN and graphene-MoS_2 heterostructures are shown in figures 8 and 9. The first four natural frequencies for graphene-hBN heterostructure are 122, 144, 187 and 202 GHz, while the corresponding values for graphene-MoS_2 heterostructure are 102, 131, 154 and 190 GHz.

For the case of graphene-hBN, first mode shape is an out of plane bending with a cantilever tip motion, second mode shape is an out of plane bending with single waviness, third mode shape is a torsional twisting mode and the fourth mode shape is an out of plane bending with double waviness. These mode shapes are comparable to that of bilayer graphene [45]. For the case of graphene-MoS_2, first mode shape is an out of plane bending with a cantilever tip motion, second mode

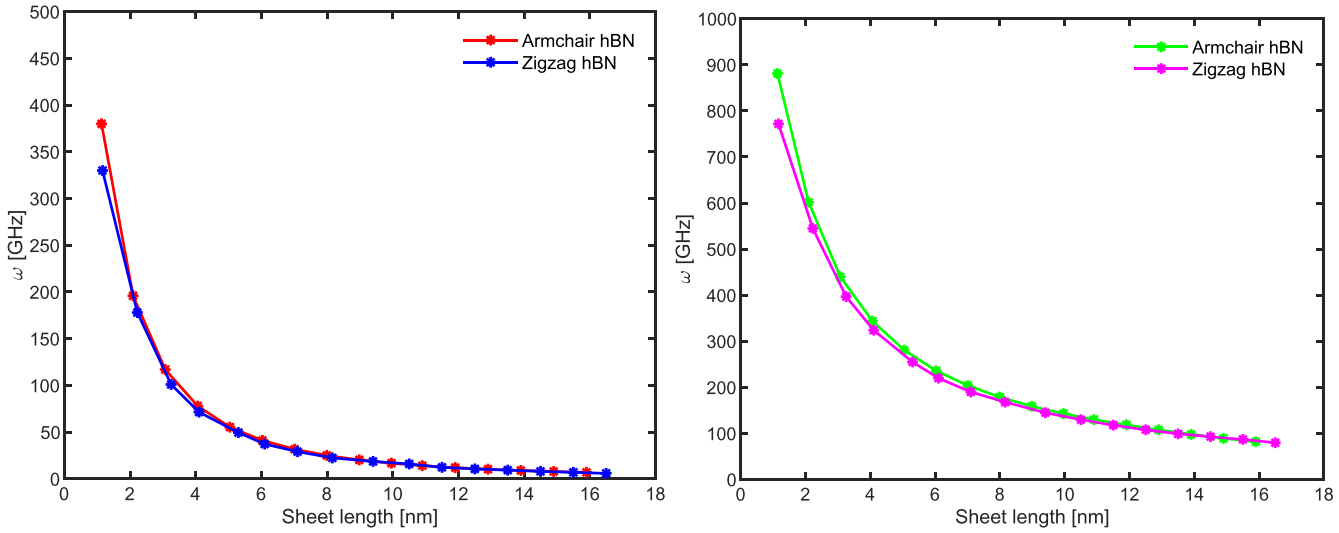

(a) Cantilever model (b) Bridged model

Figure 10. The dependence of natural frequency on sheet length: (a) Cantilevered boundary condition—fundamental natural frequency of armchair and zigzag graphene-hBN heterostructure as a function of sheet length. (b) Bridged boundary condition—fundamental natural frequency of armchair and zigzag graphene-hBN heterostructure as a function of sheet length.

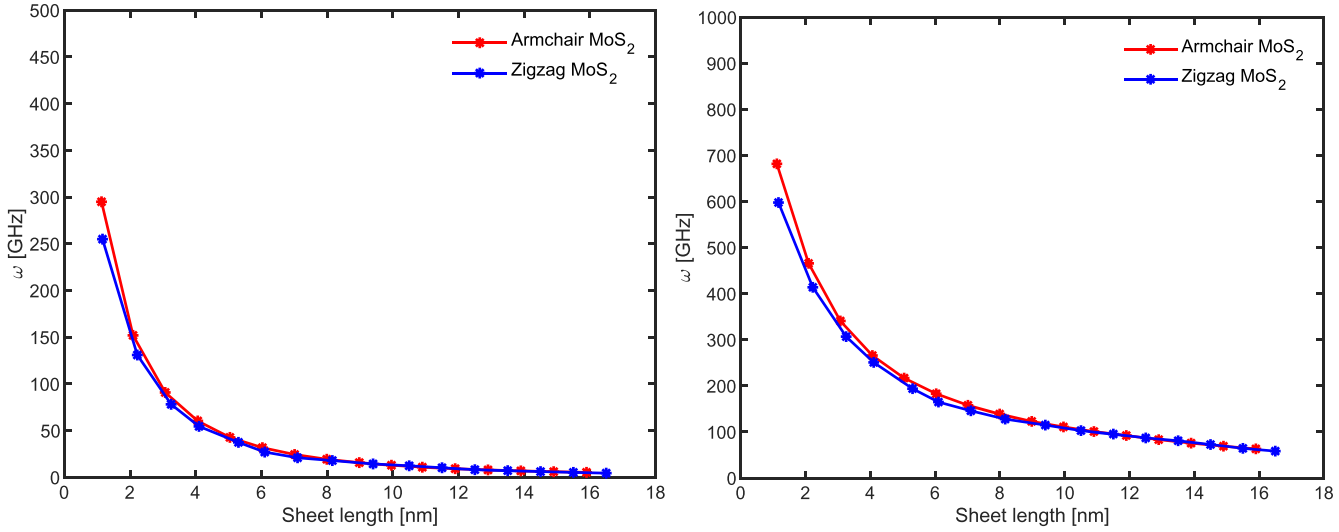

(a) Cantilever model (b) Bridged model

Figure 11. The dependence of natural frequency on sheet length: (a) Cantilevered boundary condition—fundamental natural frequency of armchair and zigzag graphene-MoS_2 heterostructure as a function of length. (b) Bridged boundary condition—fundamental natural frequency of armchair and zigzag graphene-MoS_2 heterostructure as a function of length.

shape is a non-homogenous out of plane bending, third mode shape is a non-homogenous twist and fourth mode shape is an out of plane opening mode. Importantly, inter layer penetrative waviness has been observed in the second mode shapes of graphene-MoS_2. Such a waviness and the presence of sheet separation modes (mode II, mode III and mode IV) in graphene-MoS_2, indicates that the layer-layer interaction stiffness (weak van der Waals/L–J potentials) is lower in graphene-MoS_2 as compared to graphene-hBN. Thus under a dynamic condition, the graphene-MoS_2 heterostructure shows more susceptibility to a failure following this mechanism. Interestingly, the interlayer interaction plays an important role in case of dynamic analysis of heterostructures unlike the case of static elastic analyses, where the weak van der Waals effects have negligible contribution [33]. It is important to note that the presence of out of plane bond angle (Ref figure 2 and table 1) in MoS_2 reduces the degree of interaction with any adjacent nanosheet. The first mode shapes for graphene-hBN and graphene-MoS_2 are similar. The other three higher order mode shapes for the two types of nano hetero-structures considered here differ from each other significantly. Such a difference indicate that the graphene-MoS_2 hetero-sheets are useful in nano oscillatory applications where sheet separation modes are needed.

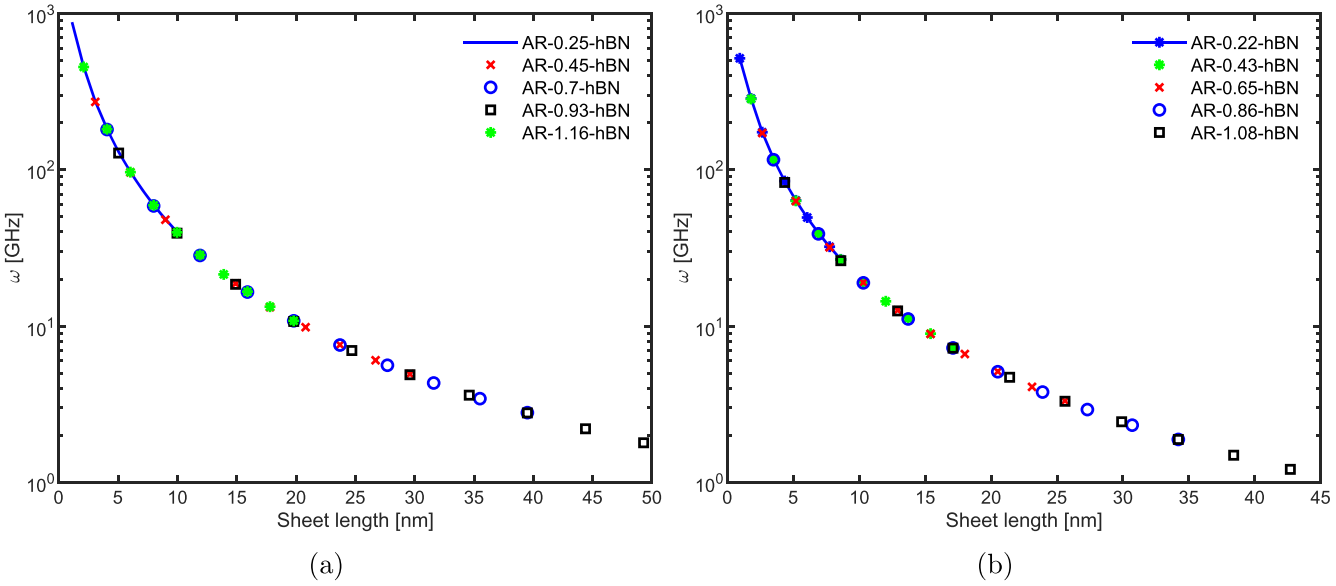

Figure 12. The variation of natural frequencies with sheet length at a given aspect ratio for graphene-hBN nano-heterostructure (a) Cantilevered graphene-hBN in armchair direction (b) Cantilevered graphene-hBN in zigzag direction.

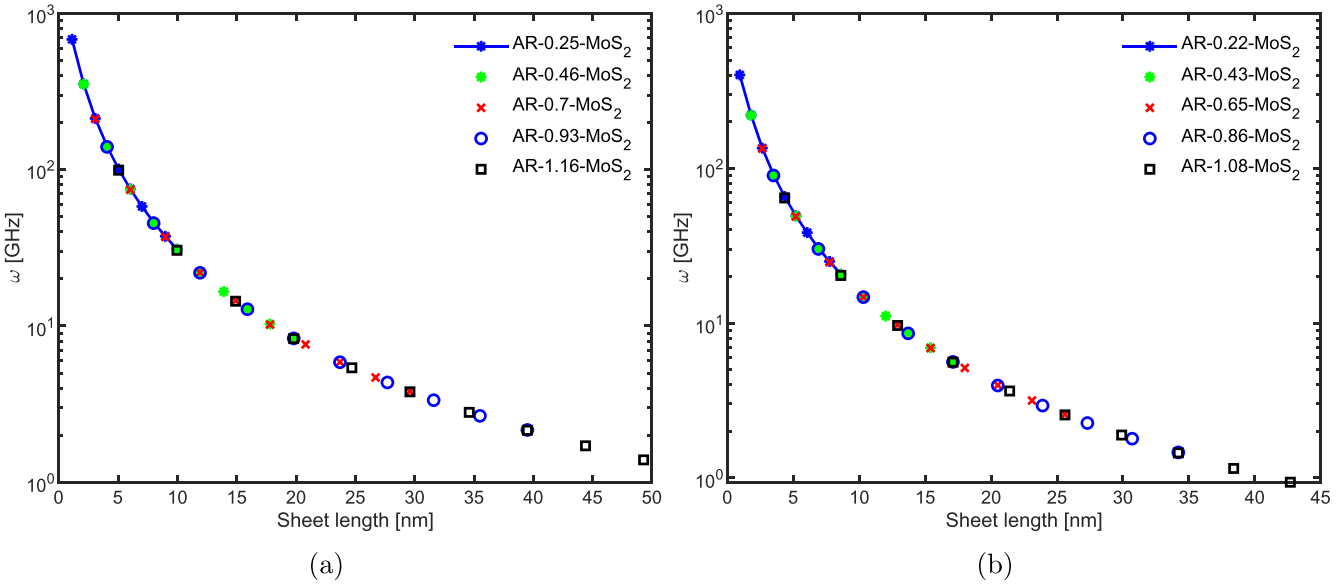

Figure 13. The variation of natural frequencies with sheet length at a given aspect ratio for graphene-MoS_2 nano-heterostructure (a) Cantilevered graphene-Mos_2 in armchair direction (b) Cantilevered graphene-MoS_2 in zigzag direction.

4.4. Size-dependence in natural frequency of nano-heterostructures

In this section, we investigate the effect of size of nanosheets on the first natural frequencies of heterostructures considering different boundary conditions with varying length. The results of fundamental natural frequency of armchair and zigzag graphene-hBN heterostructure is presented in figure 10, for bridged and cantilevered boundary conditions. It can be seen that for armchair graphene-hBN heterostructures (width = 4.08 nm) with the increasing length from ∼11 to ∼160 Å have fundamental frequencies in the range between 380 and 7 GHz for cantilever condition and 880–82 GHz for bridged condition. The zigzag graphene-hBN heterostructures (width = 4.1 nm) have their natural frequencies distributed between 330–5 GHz and 770–79 GHz for cantilevered and bridged boundary conditions respectively, with increasing lengths between 12 and 168 Å. The trend observed here (refer to figure 10) is similar to the one identified for single layer graphene [70] and bi layer graphene [45]. The results of the fundamental frequencies of armchair and zigzag graphene-MoS_2 are presented in figure 11, for bridged and cantilevered boundary conditions. It can be seen that for armchair graphene-MoS_2 heterostructures (width = 4.08 nm) with the increasing length from ∼11 to ∼160 Å have fundamental frequencies in the range between 296 and 5 GHz for cantilever condition and 680–63 GHz for bridged condition; while the zigzag graphene-MoS_2 (width = 4.1 nm) have

instead their natural frequencies distributed between 255–4 and 598–58 GHz for cantilevered and bridged boundary conditions respectively, with increasing lengths between 12 and 168 Å. The trend observed (refer to figure 10) is again similar to the one identified for single layer graphene [70] and double layer graphene [45]. In general it can be concluded that an increase in sheet length leads to a reduction in natural frequency.

In figures 12 and 13, the variations of natural frequencies for graphene-hBN and graphene-MoS_2 heterostructures with respect to length at a given AR are presented. The pattern of variation here is qualitatively similar to that of single [70] and double layer [45] graphene. This is due to the fact that all nano sheets considered are 2D in nature and they have hexagonal cells. It can be observed from the figures that sheet length has a significantly more predominant effect on the natural frequency compared to AR. As per figures 12 and 13, increase in sheet AR by keeping the sheet length constant will not lead to a significant change in natural frequency. In general, it is observed that graphene-hBN nano hetero-structure offers higher natural frequency as compared to graphene-MoS_2 for a given length and AR. This behaviour is in agreement with the stiffness (tensile rigidities) of nanosheets presented in figure 5.

4.5. Dependence on the boundary condition

From the point of view of structural mechanics, a bridged structure is found to offer higher natural frequency [71] compared to the cantilever one due to more stiffness in the system. As per figures 10 and 11, the change of the boundary condition from one-edge-fixed to both-edge-fixed can enhance the natural frequency by upto 3 times. Such a boundary condition dependence was observed for the higher natural frequencies of both graphene-hBN and graphene-MoS_2. Clamping the nano-heterostructure sheet at all edges will further enhance the stiffness, and subsequently increase the natural frequencies. Further, our study reveals that, as the AR is increased, the natural frequency of a cantilever model drops at higher rate as compared to a bridged model. From these observations, we can also conclude that the bridged topologies (refer to figure 7) are suitable for nanoelectromechanical system applications, where resonant frequencies are required to be very high, while the cantilever topologies (refer to figure 7) are suitable for low resonant frequency applications.

4.6. Effect of chirality on the natural frequencies of heterostructures

From the results presented in the preceding subsections, it can be observed that chirality is an influential factor for the natural frequencies of vibration (refer to figures 10 and 11). For a given width and length, the fundamental frequencies of armchair nano-heterostructure sheets are higher than those of zigzag ones. This difference can be attributed to the higher tensile rigidity in the armchair direction for graphene, as shown in figure 5. The maximum relative difference calculated as $(\omega_{armchair} - \omega_{zigzag})/\omega_{armchair}$ is found to be in the order of 0.14 and 0.12 for cantilevered and bridged boundary conditions, respectively. A similar trend can also be noticed from figures 12–13 for the zigzag and armchair directions. However, increasing the sheet length diminishes the difference caused by chirality. In other words, there is a size effect on the effect of chirality and it is more prominent for nanosheets with smaller dimension.

5. Summary and perspective

The area of two-dimensional (2D) materials, which started with the synthesis of graphene, has received a wide range of attention from the engineering and science community. After several years of intensive investigation, research concerning graphene has logically reached to a rather matured stage. Thus, investigation of other two-dimensional and quasi-two-dimensional materials have started receiving the due attention recently. However, the possibility of combining single layers of different two-dimensional materials (heterostructures) has expanded this field of research dramatically; well beyond the scope of considering a simple single layer graphene or other 2D material. The interest in such heterostructures is growing very rapidly with the advancement of synthesizing such materials in laboratory, as the interest in graphene did few years ago. The attentiveness is expected to expand further in coming years with the possibility to consider different tunable nanoelectromechanical properties of the prospective combination (single and multi-layer structures with different stacking sequences) of so many two-dimensional materials.

The current article presents an efficient atomistic finite element based modelling framework for the dynamic analysis of such nano-heterostructures. Here the contribution is two-fold: I. Insightful new results unravelling the dynamic behaviour of graphene based heterostructures including the effects of dependence on size, chirality and boundary conditions II. Development of the generic atomistic finite element framework for efficient dynamic analysis of heterostructures. The physics-based atomistic finite element framework is applicable to multiple 2D materials with any stacking sequence and number of layers. Adoption of the atomistic finite element approach instead of conventional simulation methods such as MD simulation brings significantly more computational efficiency in the analysis and the proposed approach is a panacea in situations where interatomic potentials required for carrying out MD simulations are unavailable in case of many complex heterostructures.

The unique capability of these heterostructures to achieve a range of simultaneously tunable multifunctional properties is expected to have a wide appeal across different disciplines of research concerning nanotechnology. Vibrational characteristics of nanostructures are of utmost importance in order to access their performance as structural members for adoption in nano-scale devices and systems. However, the dynamics and vibration of nano-heterostructures have not received the required attention yet. Thus, here we have focused on investigating the size-dependent dynamic

behavior of nano hetero-structures by developing a generic atomistic finite element model.

6. Conclusions

The vibrational characteristics of graphene based nano-heterostructures are investigated in this article considering the dependence on size, chirality and boundary conditions. A generic atomistic finite element based approach has been developed for the static and dynamic analysis of nano-heterostructures by considering the mechanical equivalence of atomic bonds, interlayer interactions and atomic masses. Within the atomistic finite element model, the inter atomic bonds are represented by equivalent structural beams with stretching and bending mechanisms, while the interlayer interaction between two adjacent layers are modelled using equivalent nonlinear spring elements based on L–J potentials. The atomic masses are modelled as lumped mass system in the dynamic analysis framework. The developed atomistic finite element model is validated extensively with available literature for effective elastic properties and vibrational frequencies. After gaining adequate confidence on the proposed computational model, insightful new results on dynamic properties are presented for graphene-hBN and graphene-MoS_2 heterostructures. Natural frequencies and mode shapes are investigated up to the fourth mode explaining their fundamental characteristics. The study reveals that the weak van der Waals interactions between the layers assume an important role in the dynamics of hetero-structures unlike the case of static elastic analysis. Depending on the modulus of elasticity, graphene-hBN shows a higher bending stiffness compared to graphene-MoS_2 hetero-structure, leading to higher natural frequencies. Similar to the behaviour of single and bilayer graphene sheets, the fundamental natural frequency of hetero-structures reduces with increasing length and AR. The nano hetero-structures with bridged boundary conditions are found to have higher natural frequencies compared to their cantilevered counterpart, making them more appropriate for high-resonance applications. A size effect is unravelled concerning the influence of chirality on the natural frequencies and it is found to be more prominent for nano-sheets with smaller dimension.

In summary, we have investigated the dynamic behaviour of graphene based heterostructures considering two different configurations with monoplanar and multi-planar 2D nano materials. Such graphene based heterostructures are ideal candidates for multi-synchronous modulation of a wide range properties for the application-specific requirements of various nanoelectromechanical devices and systems. In-depth characterization of the vibrational characteristics of these nano-heterostructures would assume a cardinal role in accessing their suitability as structural members for adoption in such nano-scale objects. Moreover, the generic atomistic finite element approach developed in this study would be useful to efficiently explore the dynamic properties of various other nano-heterostructures with multiple number of 2D materials and their stacking sequences in the future investigations.

Acknowledgments

TM acknowledges the additional financial support from IIT Kanpur during the period of this research work.

ORCID iDs

S Adhikari https://orcid.org/0000-0003-4181-3457

References

[1] Gan Y, Chu W and Qiao L 2003 STM investigation on interaction between superstructure and grain boundary in graphite *Surf. Sci.* **539** 120–8
[2] Novoselov K S, Geim A K, Morozov S V, Jiang D, Zhang Y, Dubonos S V, Grigorieva I V and Firsov A A 2004 Electric field effect in atomically thin carbon films *Science* **306** 666–9
[3] Balendhran S, Walia S, Nili H, Sriram S and Bhaskaran M 2015 Elemental analogues of graphene: silicene, germanene, stanene, and phosphorene *Small* **11** 640–52
[4] Xu M, Liang T, Shi M and Chen H 2013 Graphene-like two-dimensional materials *Chem. Rev.* **113** 3766–98
[5] Das S, Robinson J A, Dubey M, Terrones H and Terrones M 2015 Beyond graphene: progress in novel two-dimensional materials and van der Waals solids *Annu. Rev. Mater. Res.* **45** 1–27
[6] Zahedi R K, Shirazi A, Alimouri P, Alajlan N and Rabczuk T 2019 Mechanical properties of graphene-like BC_3; a molecular dynamics study *Comput. Mater. Sci.* **168** 1–10
[7] Geim A K and Grigorieva I V 2013 Van der Waals heterostructures *Nature* **499** 419
[8] Zhang Y J, Yoshida M, Suzuki R and Iwasa Y 2015 2d crystals of transition metal dichalcogenide and their iontronic functionalities *2D Mater.* **2** 044004
[9] Mahata A and Mukhopadhyay T 2018 Probing the chirality-dependent elastic properties and crack propagation behavior of single and bilayer stanene *Phys. Chem. Chem. Phys.* **20** 22768–82
[10] Mukhopadhyay T, Mahata A, Adhikari S and Zaeem M A 2017 Effective elastic properties of two dimensional multiplanar hexagonal nanostructures *2D Mater.* **4** 025006
[11] Balandin A A, Ghosh S, Bao W, Calizo I, Teweldebrhan D, Miao F and Lau C N 2008 Superior thermal conductivity of single-layer graphene *Nano Lett.* **8** 902–7
[12] Ball P 2016 Why nature prefers hexagons *Nautilus* (http://nautil.us/issue/35/boundaries/why-nature-prefers-hexagons)
[13] Mukhopadhyay T and Adhikari S 2016 Effective in-plane elastic properties of auxetic honeycombs with spatial irregularity *Mech. Mater.* **95** 204–22
[14] Mukhopadhyay T, Adhikari S and Batou A 2019 Frequency domain homogenization for the viscoelastic properties of spatially correlated quasi-periodic lattices *Int. J. Mech. Sci.* **150** 784–806
[15] Mukhopadhyay T and Adhikari S 2016 Free-vibration analysis of sandwich panels with randomly irregular honeycomb core *J. Eng. Mech.* **142** 06016008
[16] Mukhopadhyay T and Adhikari S 2017 Effective in-plane elastic moduli of quasi-random spatially irregular hexagonal lattices *Int. J. Eng. Sci.* **119** 142–79
[17] Mukhopadhyay T and Adhikari S 2016 Equivalent in-plane elastic properties of irregular honeycombs: an analytical approach *Int. J. Solids Struct.* **91** 169–84

[18] Mukhopadhyay T, Adhikari S and Alu A 2019 Theoretical limits for negative elastic moduli in subacoustic lattice materials *Phys. Rev.* B **99** 094108

[19] Zolyomi V, Wallbank J R and Falko V I 2014 Silicane and germanane: tight-binding and first-principles studies *2D Mater.* **1** 011005

[20] Lorenz T, Joswig J-O and Seifert G 2014 Stretching and breaking of monolayer MoS_2-an atomistic simulation *2D Mater.* **1** 011007

[21] Liu F, Ming P and Li J 2007 *Ab initio* calculation of ideal strength and phonon instability of graphene under tension *Phys. Rev.* B **76** 064120

[22] Grantab R, Shenoy V B and Ruoff R S 2010 Anomalous strength characteristics of tilt grain boundaries in graphene *Science* **330** 946–8

[23] Bucholz E W and Sinnott S B 2012 Mechanical behavior of MoS_2 nanotubes under compression, tension, and torsion from molecular dynamics simulations *J. Appl. Phys.* **112** 123510

[24] Bucholz E W and Sinnott S B 2013 Structural effects on mechanical response of MoS_2 nanostructures during compression *J. Appl. Phys.* **114** 034308

[25] Chang T and Gao H 2003 Size-dependent elastic properties of a single-walled carbon nanotube via a molecular mechanics model *J. Mech. Phys. Solids* **51** 1059–74

[26] Scarpa F, Adhikari S and Phani A S 2009 Effective elastic mechanical properties of single layer graphene sheets *Nanotechnology* **20** 065709

[27] Shokrieh M M and Rafiee R 2010 Prediction of Young's modulus of graphene sheets and carbon nanotubes using nanoscale continuum mechanics approach *Mater. Des.* **31** 790–5

[28] Boldrin L, Scarpa F, Chowdhury R and Adhikari S 2011 Effective mechanical properties of hexagonal boron nitride nanosheets *Nanotechnology* **22** 505702

[29] Chandra Y, Chowdhury R, Adhikari S and Scarpa F 2011 Elastic instability of bilayer graphene using atomistic finite element *Physica* E **44** 12–6

[30] Chandra Y, Chowdhury R, Scarpac F, Adhikarib S, Sienza J, Arnoldd C, Murmu T and Boulda D 2012 Vibration frequency of graphene based composites: a multiscale approach *Mater. Sci. Eng.* B **177** 303–10

[31] Mukhopadhyay T and Adhikari S 2017 Stochastic mechanics of metamaterials *Compos. Struct.* **162** 85–97

[32] Mukhopadhyay T, Adhikari S and Alu A 2019 Probing the frequency-dependent elastic moduli of lattice materials *Acta Mater.* **165** 654–65

[33] Mukhopadhyay T, Mahata A, Adhikari S and Zaeem M A 2017 Effective mechanical properties of multilayer nano-heterostructures *Sci. Rep.* **7** 15818

[34] Mukhopadhyay T, Mahata A, Adhikari S and Asle Zaeem M 2018 Probing the shear modulus of two-dimensional multiplanar nanostructures and heterostructures *Nanoscale* **10** 5280–94

[35] Jiang J-W and Park H S 2014 Mechanical properties of MoS_2/graphene heterostructures *Appl. Phys. Lett.* **105** 033108

[36] Elder R M, Neupane M R and Chantawansri T L 2015 Stacking order dependent mechanical properties of graphene/ MoS_2 bilayer and trilayer heterostructures *Appl. Phys. Lett.* **107** 073101

[37] Wei A, Li Y, Datta D, Guo H and Lv Z 2017 Mechanical properties of graphene grain boundary and hexagonal boron nitride lateral heterostructure with controlled domain size *Comput. Mater. Sci.* **126** 474–8

[38] Li Y, Zhang W, Guo B and Datta D 2017 Interlayer shear of nanomaterials: graphenegraphene, boron nitrideboron nitride and grapheneboron nitride *Acta Mech. Solida Sin.* **30** 234–40

[39] Barrios-Vargas J E, Mortazavi B, Cummings A W, Martinez-Gordillo R, Pruneda M, Colombo L, Rabczuk T and Roche S 2017 Electrical and thermal transport in coplanar polycrystalline graphenehbn heterostructures *Nano Lett.* **17** 1660–4

[40] Zhang J 2019 Vibrations of van der waals heterostructures: a study by molecular dynamics and continuum mechanics *J. Appl. Phys.* **125** 025113

[41] Gelin B 1994 *Molecular Modeling of Polymer Structures and Properties* (Munich: Hanser Gardner Publications)

[42] Chandra Y, Scarpa F, Chowdhury R, Adhikari S and Sienz J 2013 Multiscale hybrid atomistic-FE approach for the nonlinear tensile behaviour of graphene nanocomposites *Composites* A **46** 147–53

[43] Chandra Y, Scarpa F, Adhikari S, Zhang J, Flores E S and Peng H-X 2016 Pullout strength of graphene and carbon nanotube/epoxy composites *Composites* B **102** 1–8

[44] Chandra Y, Flores E S, Scarpa F and Adhikari S 2016 Buckling of hybrid nano composites with embedded graphene and carbon nanotubes *Physica* E **83** 434–41

[45] Chandra Y, Chowdhury R, Scarpa F and Adhikaricor S 2011 Vibrational characteristics of bilayer graphene sheets *Thin Solid Films* **519** 6026–32

[46] Optistruct 14.0 reference guide, Altair Engineering, Inc.

[47] Scarpa F, Adhikari S and Chowdhury R 2010 The transverse elasticity of bilayer graphene *Phys. Lett.* A **374** 2053–7

[48] Girifalco L A, Hodak M and Lee R S 2000 Carbon nanotubes, buckyballs, ropes, and a universal graphitic potential *Phys. Rev.* B **62** 13104–10

[49] Pak A J and Hwang G S 2016 Theoretical analysis of thermal transport in graphene supported on hexagonal boron nitride: the importance of strong adhesion due to π-bond polarization *Phys. Rev. Appl.* **6** 034015

[50] Neek-Amal M and Peeters F M 2014 Graphene on boron-nitride: Moir pattern in the van der Waals energy *Appl. Phys. Lett.* **104** 041909

[51] Montgomery P L 1995 A block Lanczos algorithm for finding dependencies over GF(2) *Advances in Cryptology–EUROCRYPT '95* ed L C Guillou and J-J Quisquater (Berlin: Springer) pp 106–20

[52] Demczyk B, Wang Y, Cumings J, Hetman M, Han W, Zettl A and Ritchie R 2002 Direct mechanical measurement of the tensile strength and elastic modulus of multiwalled carbon nanotubes *Mater. Sci. Eng.* A **334** 173–8

[53] Song L *et al* 2010 Large scale growth and characterization of atomic hexagonal boron nitride layers *Nano Lett.* **10** 3209–15

[54] Bertolazzi S, Brivio J and Kis A 2011 Stretching and breaking of ultrathin MoS_2 *ACS Nano* **5** 9703–9

[55] Lee C, Wei X, Kysar J W and Hone J 2008 Measurement of the elastic properties and intrinsic strength of monolayer graphene *Science* **321** 385–8

[56] Kudin K N, Scuseria G E and Yakobson B I 2001 c_2F, BN, and C nanoshell elasticity from *ab initio* computations *Phys. Rev.* B **64** 235406

[57] Lier G V, Alsenoy C V, Doren V V and Geerlings P 2000 *Ab initio* study of the elastic properties of single-walled carbon nanotubes and graphene *Chem. Phys. Lett.* **326** 181–5

[58] Sánchez-Portal D, Artacho E, Soler J M, Rubio A and Ordejón P 1999 *Ab initio* structural, elastic, and vibrational properties of carbon nanotubes *Phys. Rev.* B **59** 12678–88

[59] Jiang J-W, Wang J-S and Li B 2009 Young's modulus of graphene: a molecular dynamics study *Phys. Rev.* B **80** 113405

[60] Zhao H, Min K and Aluru N R 2009 Size and chirality dependent elastic properties of graphene nanoribbons under uniaxial tension *Nano Lett.* **9** 3012–5

[61] Peng Q, Ji W and De S 2012 Mechanical properties of the hexagonal boron nitride monolayer: *ab initio* study *Comput. Mater. Sci.* **56** 11–7

[62] Zhao S and Xue J 2013 Mechanical properties of hybrid graphene and hexagonal boron nitride sheets as revealed by molecular dynamic simulations *J. Phys. D: Appl. Phys.* **46** 135303

[63] Le M-Q 2014 Young's modulus prediction of hexagonal nanosheets and nanotubes based on dimensional analysis and atomistic simulations *Meccanica* **49** 1709–19

[64] Jiang L and Guo W 2011 A molecular mechanics study on size-dependent elastic properties of single-walled boron nitride nanotubes *J. Mech. Phys. Solids* **59** 1204–13

[65] Oh E-S 2011 Elastic properties of various boron-nitride structures *Met. Mater. Int.* **17** 21–7

[66] Castellanos-Gomez A, Poot M, Steele G A, van der Zant H S J, Agrat N and Rubio-Bollinger G 2012 Elastic properties of freely suspended MoS_2 nanosheets *Adv. Mater.* **24** 772–5

[67] Lorenz T, Teich D, Joswig J-O and Seifert G 2012 Theoretical study of the mechanical behavior of individual TiS_2 and MoS_2 nanotubes *J. Phys. Chem.* C **116** 11714–21

[68] Scalise E, Houssa M, Pourtois G, Afanas'ev V and Stesmans A 2012 Strain-induced semiconductor to metal transition in the two-dimensional honeycomb structure of MoS_2 *Nano Res.* **5** 43–8

[69] Jiang J-W, Qi Z, Park H S and Rabczuk T 2013 Elastic bending modulus of single-layer molybdenum disulfide (MoS_2): finite thickness effect *Nanotechnology* **24** 435705

[70] Sakhaee-Pour A, Ahmadian M T and Naghdabadi R 2008 Vibrational analysis of single-layered graphene sheets *Nanotechnology* **19** 085702

[71] Warburton G B 1954 The vibration of rectangular plates *Proc. Inst. Mech. Eng.* **168** 371–84

[72] Li C and Chou T-W 2003 A structural mechanics approach for the analysis of carbon nanotubes *Int. J. Solids Struct.* **40** 2487–99

[73] Gupta K K, Mukhopadhyay T, Roy A and Dey S 2020 Probing the compound effect of spatially varying intrinsic defects and doping on mechanical properties of hybrid graphene monolayers *J. Mater. Sci. Techmol.* at press